energies

MDPI

Article

The Comparative Analysis of Phase Shifting Transformers

Paweł Albrechtowicz * and Jerzy Szczepanik

Department of Electrical Engineering, Cracow University of Technology, Warszawska 24 St., 31-155 Cracow, Poland; jszczepanik@pk.edu.pl

* Correspondence: pawel.albrechtowicz@pk.edu.pl

Abstract: Phase shifting transformers (PSTs) are currently widely used in power systems to control power flow. In this manuscript, the results of the asymmetrical PST (APST) with the in-phase PST (called asymmetrical controllable PST-ACPST) were compared, allowing to control both longitudinal and quadrature voltage. The MATLAB simulation model of the ACPST was built to obtain influence of PST in selected models for selected parameters. Then the 30A laboratory PST device was built in the laboratory. The parameters of the MATLAB model were then adjusted to parameters of the real life PST model. This allowed verifying the results of the real life and computer simulations. Based on the ACPST simulation model, the APST model was built; for the given work conditions, the influence of both PSTs were compared. APST construction always resulted in higher output voltage than the input one. ACPST achieved the same power transfer for the lower output PST voltage, which is its main advantage. This dependency is a result of the greater ACPST angle compared to the classical APST. The ACPST also allowed adjusting longitudinal and quadrature voltages; therefore, this PST type can be installed in places where high flexibility is required, especially in systems with high renewable energy sources penetration.

Keywords: phase shifting transformer; transmission line; power system

Citation: Albrechtowicz, P.; Szczepanik, J. The Comparative Analysis of Phase Shifting Transformers. *Energies* **2021**, *14*, 4347. https://doi.org/10.3390/en14144347

Academic Editor: Andrea Mariscotti

Received: 8 June 2021
Accepted: 18 July 2021
Published: 19 July 2021

1. Introduction

Phase shifting transformers (PSTs) are some of the key devices used nowadays for power flow control in distribution power supply networks (PSN). When the optimal power flow is provided, the system operates at the best possible technical and economic parameters (minimum transmission losses, stability reserve). Emphasis on installing power flow controlling equipment in PSN will increase, as the size, amount of transmitted power, and penetration by distributed and turbulent sources (wind generation) increases. The technical developments in transmission grids (microgrids, smart grids), aimed at their optimization and better utilization, increases the demand for Flexible Alternating Current Transmission System (FACTS) class devices [1–5], including power flow controlling equipment. In Europe, there are unsolved complications with the power flow control via interconnection lines between two transmission systems operators (two countries). Unplanned and uncontrollable power flows (for example, flows between Poland and Germany) cause changes in working points of both systems planned together during trade operations [6–8]. In the western part of Europe, some of the problems with power flow control can be visible in the Benelux region [9,10], where PSTs have to be installed to control power flow distributions caused by wind farms [11]. Central–east Europe shows unplanned power flow from Germany to Poland, then to the Czech Republic (or Slovakia), and Austria [12,13]. For many years, PSTs were used to prevent cases of unscheduled power flow in some interconnected transmission power lines. However, as the number of grid interconnections increases, the new applications of PSTs in the European power systems will also increase. As expressed in [14], the number of PST investments is equal to 7. TYNDP reports [15,16] describe PSTs under construction, planning phase, or under consideration, in many locations, especially in Germany in the 2025 or 2030 time horizon.

High powers transferred via PSTs and the significance of their roles in the integrated power systems results in high requirements, concerning reliability in their functioning and control arrangements. The natural consequence of the construction and operational requirements is a high price for each PST unit.

Despite well-known PST constructions functioning on the market, there is still a need to search for better solutions to improve PST structure, work, and control procedures [17].

This paper presents simulations and laboratory model research for proposed PST structure and transformer winding arrangements. The laboratory set-up of the PST was applied to the laboratory models of the power systems supplied from two different low voltage subsystems.

The main contribution of the presented can be expressed as:

1. Presentation of the working idea of asymmetrical phase shifting transformer;
2. Verification of the laboratory test, simulation comparison of the proposed solution with classical asymmetrical phase shifting transformers.

The article is organized as follows: Section 2 describes the power flow control theoretical analysis. Section 3 describes asymmetrical phase shifting transformers (classical and proposed by authors). Section 4 concerns laboratory set-up; Section 5 presents the laboratory measurements; Section 6 compares the classical and proposed PST simulation results; and the final section presents the conclusion.

2. Power Flow Control in the Power Systems

This article presents an analysis of the power flow through the transmission line connecting two systems or two subsystems. The analysis includes extra voltage added at the beginning of the line to observe the influence of the power flow for different line lengths (different line impedances) and variable internal system impedances. The behavior of the analyzed system can be illustrated as a simple scheme presented in Figure 1

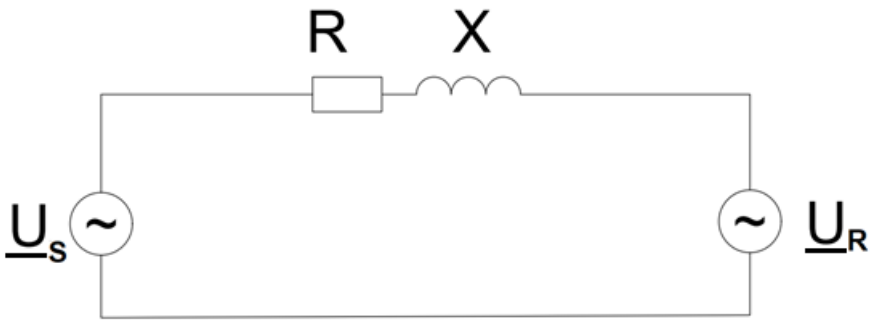

Figure 1. Simplified electrical scheme of the systems connected through the II-type line.

The system simplification leads to the equivalent circuit consisting of two sources connected by impedance (Figure 2). For the second-order line model, this impedance consists only of resistance and reactance. It is obvious that line current depends on voltage difference at the line ends and line parameters. Thus, the line power flow is defined for the linear system (it is also voltage-dependent). In the case of the supply line, loaded only by the passive load, the voltage depends on voltage and voltage drop on the supply line caused by the load current. For the line connecting two systems, voltage difference and line parameters determine the line current.

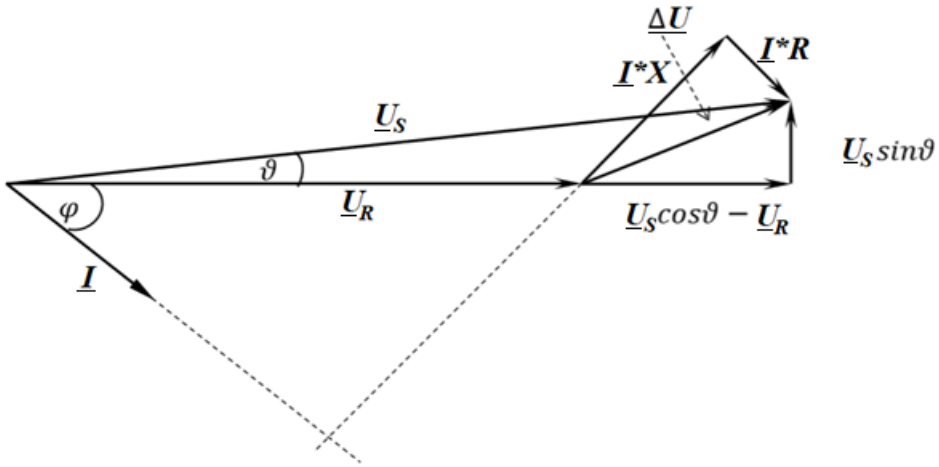

Figure 2. Phasor diagram for the transmission line from the Figure 1.

The result of the current flow through the elements R and X is the voltage loss, which is equal to the voltage difference between line ends [17–20].

$$\underline{\Delta U} = (R + jX) \cdot \underline{I} \tag{1}$$

From phasor diagram (Figure 2) voltage the voltage loss can be derived as:

$$\Delta U = U_S cos(\vartheta) - U_R + jU_S sin(\vartheta) \tag{2}$$

when Formula (1) is used to calculate the current, considering Formula (2), the formula showing dependence of line power flow on values and the angle of the line end voltages can be derived.

$$\mathrm{S} = U_R \frac{R(U_S cos\vartheta - U_R) + XU_S sin\vartheta + j(RU_S sin\vartheta - XU_S cos\vartheta - U_R)}{R^2 + X^2} \tag{3}$$

Further simplification is possible, where $X/R > 7$, and due to the square relationship, the value of R can be omitted. This happens in the case of HV lines; thus, relationship 4 can be rewritten as:

$$S = \frac{U_S U_R}{X} sin\vartheta + j\frac{U_S U_R}{X}\left(cos\vartheta - \frac{U_R}{U_S}\right) \tag{4}$$

According to a relationship (4), the increase of active power transfer is possible by increasing angle ϑ, increasing the value of voltages, or decreasing line reactance. At the same time, as angle ϑ grows, the active power flow also grows. When angle ϑ is regulated close to "0", the regulation of active power flow is much faster than reactive flow (see the properties of functions sine and cosine). The regulation of angle ϑ is now possible using phase shifters, power shift transformers (PST), and UPFC or DC link-based devices. The research in this article concentrates on the devices that change the angle and value of the line sending end, via application of additional voltage sources, for example, PST or UPFC.

3. Phase Shifting Transformers

Phase shifting transformers are well known devices used to control power flow in power systems worldwide. Through the years, different constructions with elementary divisions were invented [9,10,21,22]:

- Symmetrical;
- Asymmetrical;
- Independent.

According to the construction:

- Single-core;
- Two-core.

Figure 3 shows a schematic diagram of selected phase shifting transformers. According to [23,24], it is possible to obtain maximal PST parameters:

- Rated through put power up to 1800 MVA;
- Rated voltage up to 765 kV;
- Maximum no-load phase angle up to ±85°.

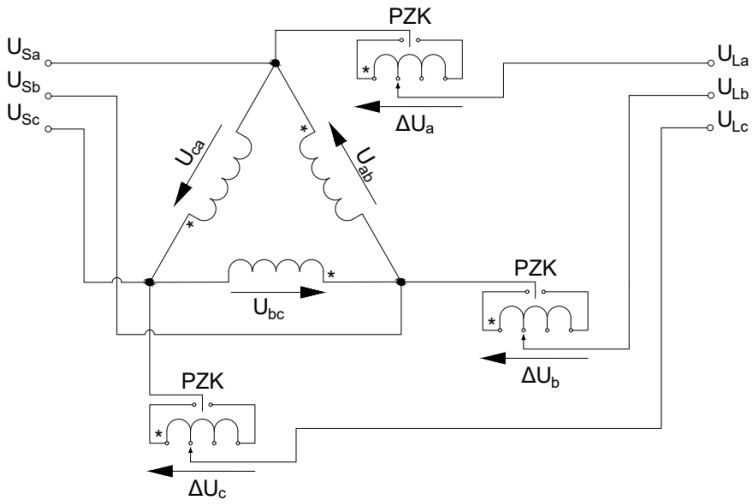

Figure 3. Asymmetrical single core PST scheme.

Comparing PST types, features can be highlighted according to construction. For example, single-core units have smaller maximal possible phase shift adjustments compared to dual-core PST construction [25], but they are less expensive [24]. Because of the regulation and connection PST types, symmetrical units can only control active power, while asymmetrical and independent control systems allow both active and reactive power regulation [25].

3.1. Asymmetrical Phase Shifting Transformer (APST)

Asymmetrical PST allows changing both the phase and magnitude of the output voltage concerning the input voltage. One can notice that there will always be greater output voltage than the input one, which results from the APST principles [22,23,26]. The phasor diagram of the APST and the voltage dependency is presented in Figure 4.

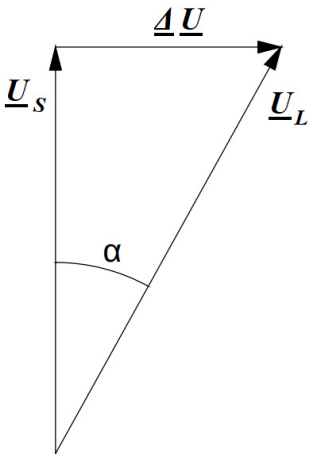

Figure 4. APST voltage phasor diagram.

To the input voltage U_S is added the quadrature voltage ΔU, and as a consequence of this operation, the output voltage U_L is obtained. In this way, an angle α is implemented. Due to this, there is the possibility of achieving an active power increment or decrement (depending on the additional voltage direction—retard or advance).

The active power curve and angle α versus the quadrature voltage are shown in Figure 5.

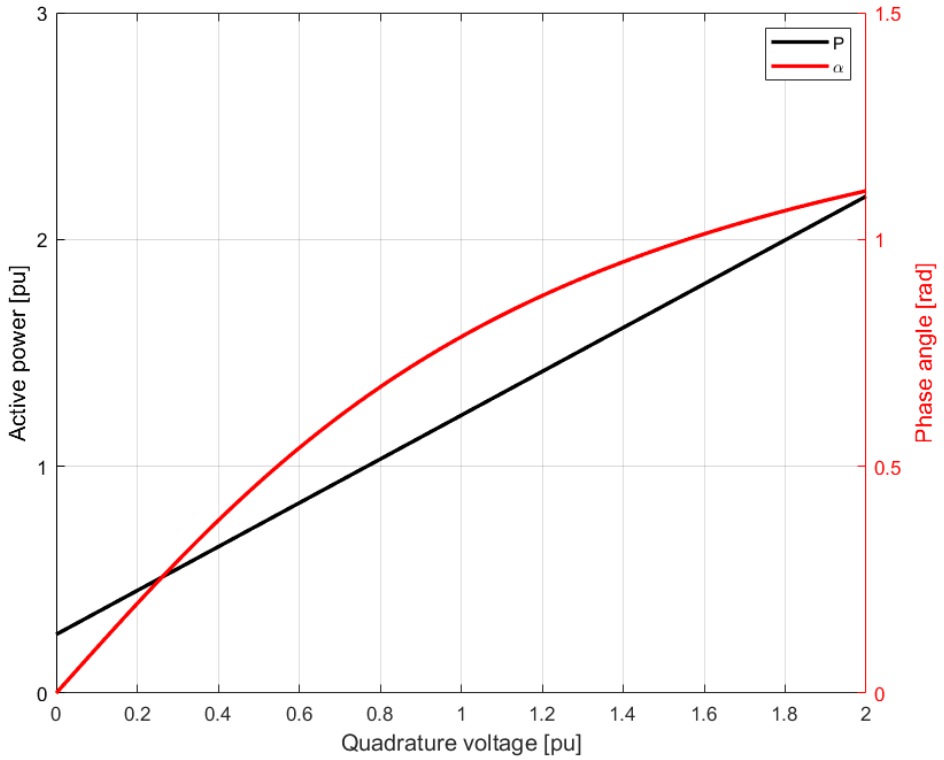

Figure 5. APST theoretical active power and phase angle curves.

Using the phasor diagram from Figure 4, the α angle in the ideal direct asymmetrical PST can be expressed:

$$\alpha = arctg\left(\frac{\Delta U}{U_S}\right) \tag{5}$$

Then, the transmitted active power is equal to:

$$P = \frac{U_L U_R}{X} sin(\delta + \alpha) \tag{6}$$

Finally, using trigonometric dependencies, the active power transmitted is obtained according to Equation (7):

$$P = \frac{U_R}{X}(U_S sin\delta + \Delta U cos\delta) \tag{7}$$

3.2. Asymmetrical Controllable Phase Shifting Transformers (ACPST)

PST construction, proposed in this paper, is similar to conventional APST. The main advantage of the authors' device is the possibility of adjusting voltage U_S. In this way, the α angle can achieve higher values without increasing PST output voltage. Moreover, ACPST can be controlled to obtain the same output voltage magnitude compared to the input one.

The phasor diagram visible in Figure 6 represents the possible state of voltages in ACPST.

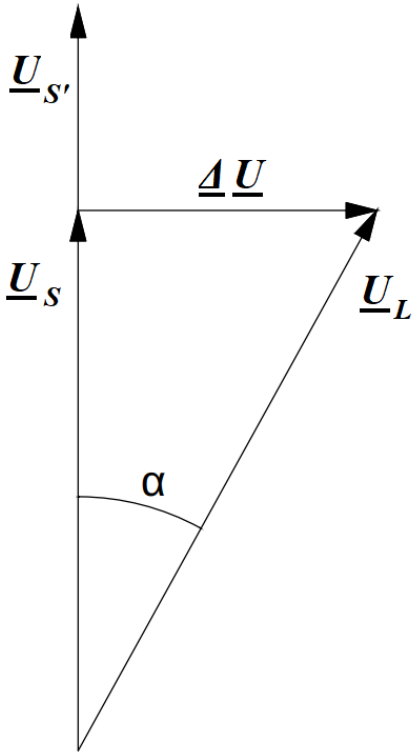

Figure 6. ACPST voltage phasor diagram.

Input voltage U_S is lowered (or can be increased) by the transformer tap changer and adjusted to the given voltage level. The analysis can be implemented by transformer ratio ϑ:

$$\vartheta = \frac{U_S{}'}{U_S} \tag{8}$$

In this way, it can be rewritten as the transmitted active power:

$$P = \frac{U_R}{X}\left(\frac{U_S{}'}{\vartheta} sin\delta + \Delta U cos\delta\right) \tag{9}$$

Equation (9) is very similar to Equation (7), but there is additional elements, considering input voltage regulation—transformer ratio ϑ. For this reason, there can be regulated both vectors, U_S and ΔU respectively. An impact of input voltage regulation is presented in Figure 7.

The obtained theoretical active power waveform shows that the decreased input voltage, Us, to the 95% nominal voltage, achieved a lower active power transmission compared to the nominal voltage and increased input voltage Us to the 105% nominal one. In some conditions, it is beneficial to lower the input voltage Us and add quadrature voltage to achieve a greater angle α keeping, e.g., constant output voltage UL compared to the line voltage Us'.

The ACPST can be properly controlled by choosing any objective function, e.g., maintaining the output ACPST voltage at the given constant level or for a constant angle α. An example with a comparison of the values for two different control types is presented in Table 1.

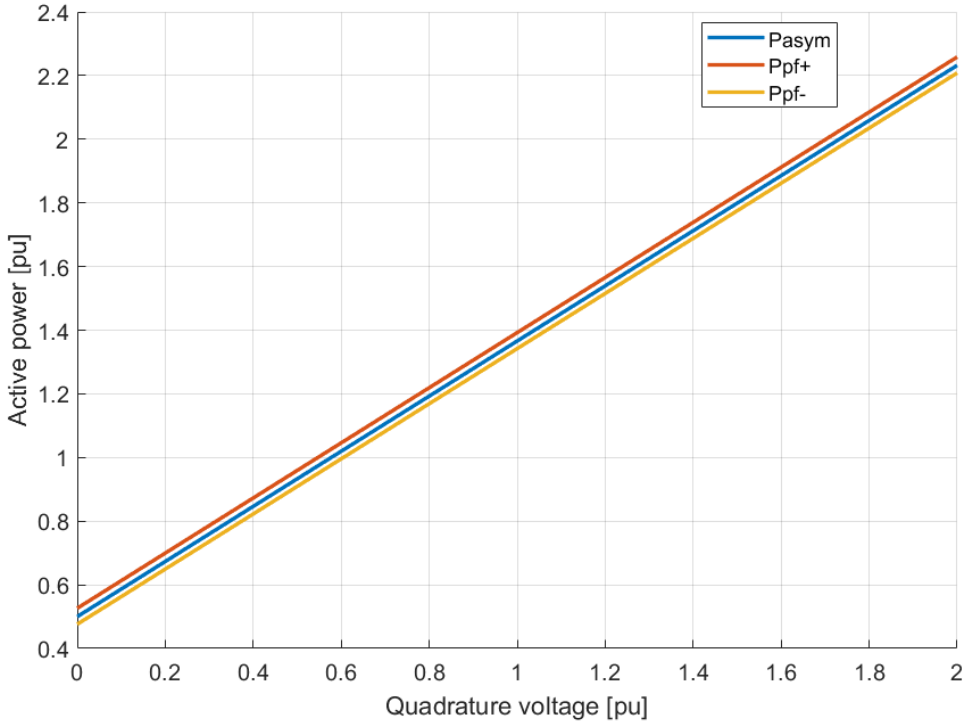

Figure 7. ACPST active power curves for 105% U_n (red), U_n (blue), and 95% U_n (yellow).

Table 1. ACPST energy parameters for constant input voltage and output voltage.

U_S = const					U_L = const				
U_S (V)	α (°)	ΔU (V)	U_L (V)	ΔP (%)	U_S (V)	α (°)	ΔU (V)	U_L (V)	ΔP (%)
230	0	0	230.00	3.5	230	0	0	230	3.5
230	2	8.03	230.14	7.0	229.86	8.02	2	230	7.0
230	4	16.07	230.56	10.5	229.44	16.04	4	230	10.5
230	6	24.16	231.27	14.0	228.74	24.03	6	230	13.9
230	8	32.31	232.26	17.5	227.76	31.99	8	230	17.4
230	10	40.53	233.54	21.1	226.51	39.92	10	230	20.8
230	12	48.86	235.13	24.7	224.98	47.80	12	230	24.2
230	14	57.32	237.03	28.4	223.17	55.61	14	230	27.6
230	16	65.92	239.26	32.1	221.10	63.37	16	230	30.9
230	18	74.69	241.82	36.0	218.75	71.04	18	230	34.2
230	20	83.67	244.75	39.9	216.14	78.63	20	230	37.5
230	22	92.87	248.04	43.9	213.27	86.12	22	230	40.7
230	24	102.34	251.74	48.0	210.14	93.50	24	230	43.8
230	26	112.11	255.87	52.2	206.75	100.78	26	230	46.9
230	28	122.22	260.46	56.6	203.10	107.93	28	230	50.0
230	30	132.71	265.54	61.2	199.22	114.95	30	230	53.0
230	32	143.63	271.16	65.9	195.09	121.83	32	230	55.9

4. Laboratory Arrangement and Simulation Model

4.1. Laboratory Setup

The laboratory ACPST is composed of two special transformers. In particular, two transformers were chosen to obtain better possibilities of control and measurement availability. The first one is a controllable transformer, allowing input voltage regulation (longitudinal voltage part). It is connected into Yy. The secondary windings were divided into 15 voltage (phase to phase) levels from 340 to 430 V with the 6 V step. The second one is responsible for quadrature voltage addition (transverse voltage part), which is connected

to DIII. Three insulated secondary windings are implemented in series with each line phase. There is a possibility of getting voltages from 0 to 256 V with the 4 V steps. Such a small regulation step is selected intentionally because of different laboratory arrangements. For short transmission lines (small longitudinal line impedance)—the transmitted active power sensitivity on the quadrature voltage may be high, but then it would not be the right regulation properties. For small voltage steps, the possibility of better power flow control is more likely. An installed winding switch could change the quadrature voltage direction as well. The phasor diagram for ACPST is shown in Figure 8, presenting maximal achievable angles for two opposite longitudinal voltage values—minimal U_{Smin} equal to 196 V_{rms} (phase to ground voltage) and maximal U_{Smax} equal to 248 V_{rms}. In this way, from the ACPST, the output voltage for maximal quadrature voltage (ΔU_{max} = 256 V_{rms}) can be 322 V_{rms}, angle $\alpha_2 = 52.6^\circ$ and 356 V_{rms}, angle $\alpha_1 = 45.9^\circ$ for U_{smin} and U_{smax}, respectively. The described maximal values for such a designed phase shifting device clearly indicates a possible angle increment ($\Delta\alpha = 6.7^\circ$). Nevertheless, this fact is not the most important. The presented ACPST construction has the largest advantage in maintaining constant output voltage value compared to classical APST. Thus, in this way, it can be classified both as asymmetrical (may create an altered phase angle and magnitude of output voltage) and symmetrical (may alter the phase angle and keep a constant output voltage magnitude). Transformers data are presented in Table 2.

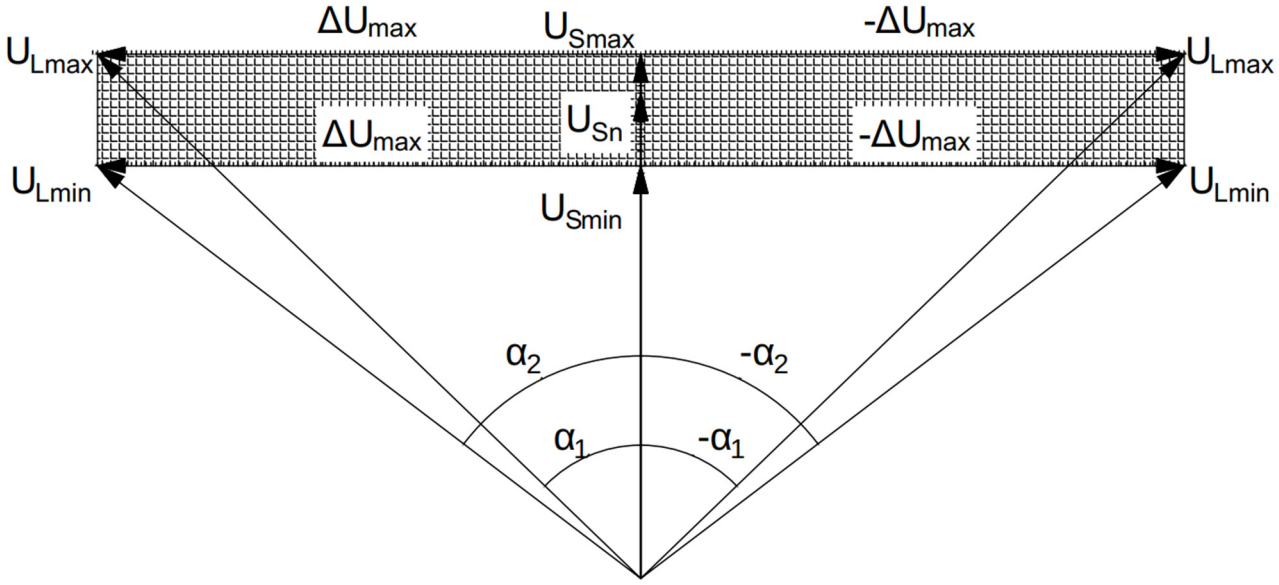

Figure 8. ACPST phasor diagram for minimal and maximal possible longitudinal voltages and maximal quadrature voltage.

Table 2. Transformers data.

	Rated Primary Voltage [V]	Rated Secondary Voltage [V]	Rated Primary Current [A]	Rated Secondary Current [A]	Rated Power [kVA]	Rated Frequency [Hz]	Connection Group	Short-Circuit Voltage [%]
Quadrature transformer	3 × 400	3 × 128/3 × 64/3 × 32/3 × 16/3 × 8/3 × 4	3 × 33.2	3 × 30/3 × 30/3 × 30/3 × 30/3 × 30	22.5	50	D/iiiiii	3.88
Longitudinal transformer	3 × 400	3 × 400 + 5 × 1.5%–10 × 1.5%	3 × 33	3 × 32.5	22.5	50	Yy0	5.10

The transmission line is divided into sections, and each section is modeled as a π-type (Figure 9). The parameters of the line are selected in this way, to achieve the model 400 kV overhead transmission line, where one section represents 30 km of a real life line [26]. The laboratory line model is made for the maximal long-lasting current 30 A, but during tests, was limited to 26 A.

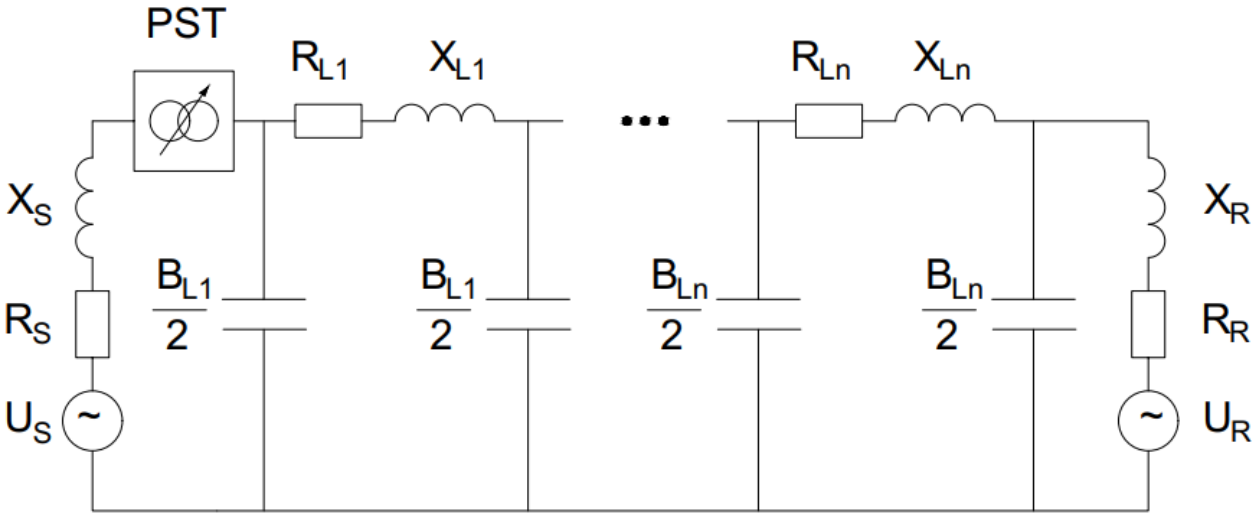

Figure 9. The laboratory system connection scheme.

Laboratory tests were carried out for the line lengths, varying from 24 sections (720 km of the line) to 4 sections (120 km of the line).

Both systems may have variable internal impedance and regulated voltage levels. For analyzed cases, there were set conditions:

- System S2 internal impedance greater than system S1 (Z_{S1} = 1.24 Ω, Z_{S2} = 0.46 Ω);
- Nominal voltage of system S1 greater than S2 (V_{S1} = 1.24 V, V_{S2} = 0.46 V);
- Phase angle between both systems voltages 0° (no load).

The measurement system consisted of current clamps (Fluke ac i1000s-measurement range 100 A, 10 mV/A, accuracy 2% of reading ±5 mV), differential voltage probes (Pintek DP-200pro, measurement range 100:1, accuracy ≤±2%), and the data acquisition system built on the NI USB-6259 measuring card and NI LabVIEW Signal Express software in ver. 15.0.0 (National Instruments Corp., Austin, TX, USA) [27,28].

4.2. Simulation Model

The simulation model was created based on the laboratory ACPST construction. All transformer parameters were put in the Simulink transformer blocks, and the laboratory power supply system parameters. The line was built as a distributed π-line model with the parameter value adequate to the laboratory setup [29].

The Simulink model arrangement is presented in Figure 10. Based on this construction, the APST was created by a by-pass on the longitudinal regulation transformer.

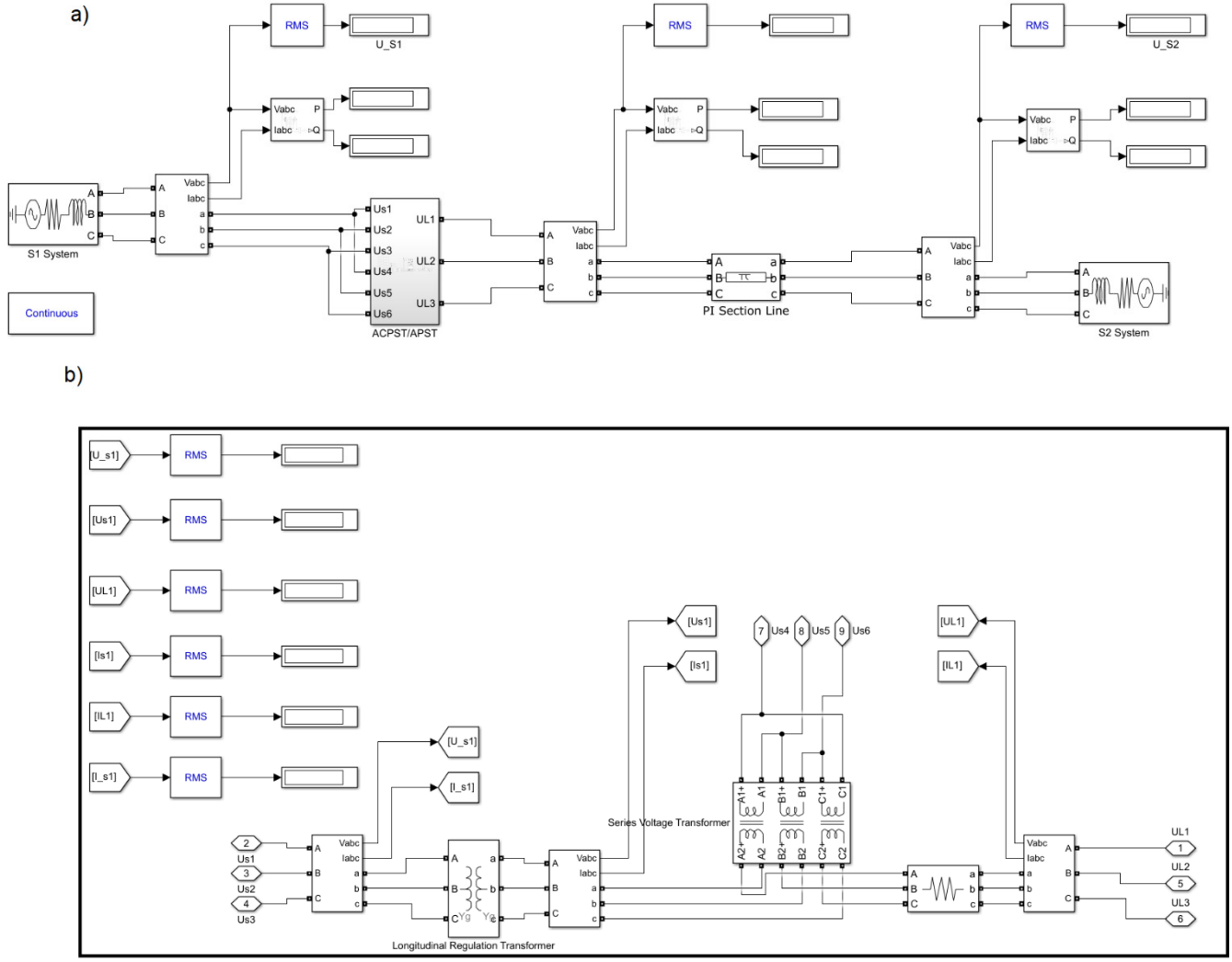

Figure 10. Simulink laboratory model equivalent, (**a**) general arrangement, (**b**) ACPST connection scheme.

5. Laboratory Tests

The laboratory research was performed considering limits described in Section 4. Figure 11 presents active powers transmitted through the ACPST and the line, from 24 sections to 4 sections from system S1 to system S2.

It is visible that the line is shorter (and so the line impedance is more negligible), the transmitted active power is higher for the start case (added quadrature voltage is 0). The dependency on the transmitted active power is clear and easy to understand. The line is longer, the higher quadrature voltage injection is needed to achieve a given power flow, which is a natural consequence of greater line impedance installed between two systems. The gradient of each transmitted active power through the varying line length in Figure 10 can be expressed using Equation (10):

$$\frac{\partial P}{\partial \Delta U} = \frac{U_R}{X_Z} cos\delta \tag{10}$$

The line is shorter; the X_Z is smaller, so the gradient is higher, because both the natural phase angle δ and the receiving end voltage UR can be assumed as constant.

In an ideal impedance-less PST will not result voltage drops on the internal impedance. However, for each real element, there must occur some voltage losses.

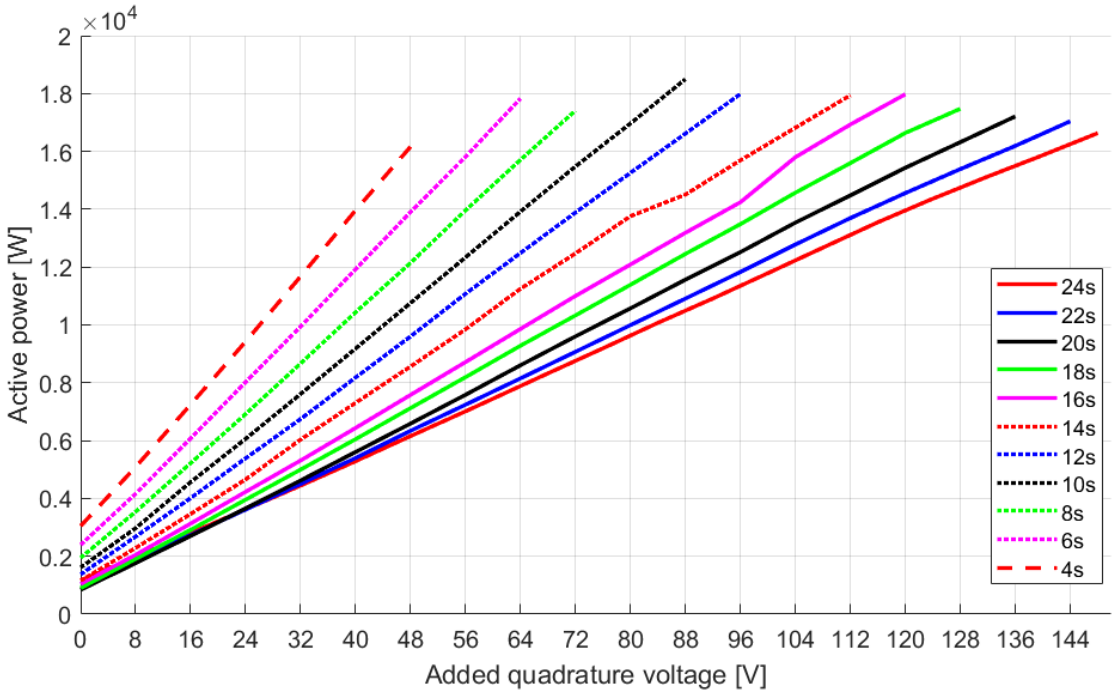

Figure 11. Active power transfer for different line lengths.

Figure 12 shows the chosen examples of the transmitted active powers for the nominal longitudinal voltage (230 V_{rms}) and the smallest possible one (196 V_{rms}) for the line with 22 sections. The longitudinal voltage difference for blue and red lines is equal to around 34 V_{rms}. However, for transmitted active power, the same power values are achievable for the red case if only there is added quadrature voltage around 8 V_{rms} more than in the blue case. What is interesting, the red case is operating on voltage values lower (213 V–238 V) than or close to the nominal line voltage (230 V) instead of higher values (234 V–255 V) for the blue one. The ACPST output voltages are shown in Table 3.

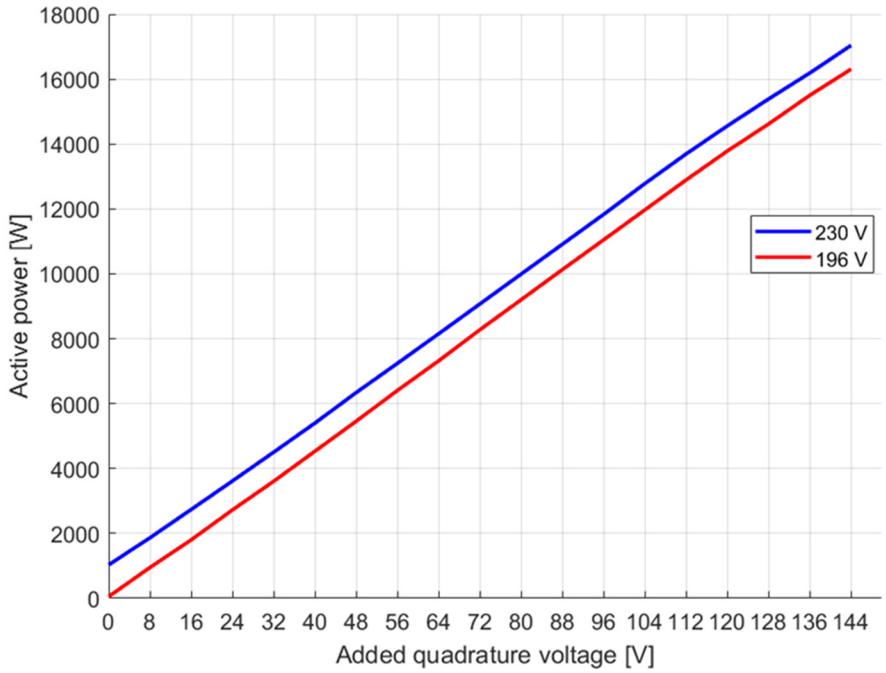

Figure 12. Active power transfer for two longitudinal voltage cases: 230 V (blue) and 196 V (red).

Table 3. The ACPST output voltages for 230 V and 196 V longitudinal voltages.

Quad. Voltage [V]	**0**	**8**	**16**	**24**	**32**	**40**	**48**	**56**	**64**	**72**
Output ACPST voltage [V] (blue case 230 V)	234.60	234.17	234.01	234.22	234.56	234.88	235.93	236.56	237.47	238.80
Output ACPST voltage [V] (red case 196 V)	213.47	213.13	212.98	213.36	213.54	214.33	215.37	216.52	217.80	219.62
Quad. Voltage [V]	**80**	**88**	**96**	**104**	**112**	**120**	**128**	**136**	**144**	
Output ACPST voltage [V] (blue case 230 V)	240.23	241.91	243.76	245.77	247.46	249.28	251.13	252.66	254.75	
Output ACPST voltage [V] (red case 196 V)	221.32	223.08	224.92	226.84	229.06	231.18	233.67	236.05	237.93	

The presented output voltage values can be taken as an important dependency for some operations in the power systems: ACPST construction allows to transmit the same active powers for the lower voltages (but for higher angle α).

Based on the nominal parameters of the transformers, given by their manufacturer, and on the measured data, authors built a simulation model in Simulink/MATLAB software. For measured laboratory system parameters and based on the manufacturers' catalogue data, simulations were performed for analogical power systems and line length scenarios. Figure 13 presents active power transfers for simulations and laboratory tests.

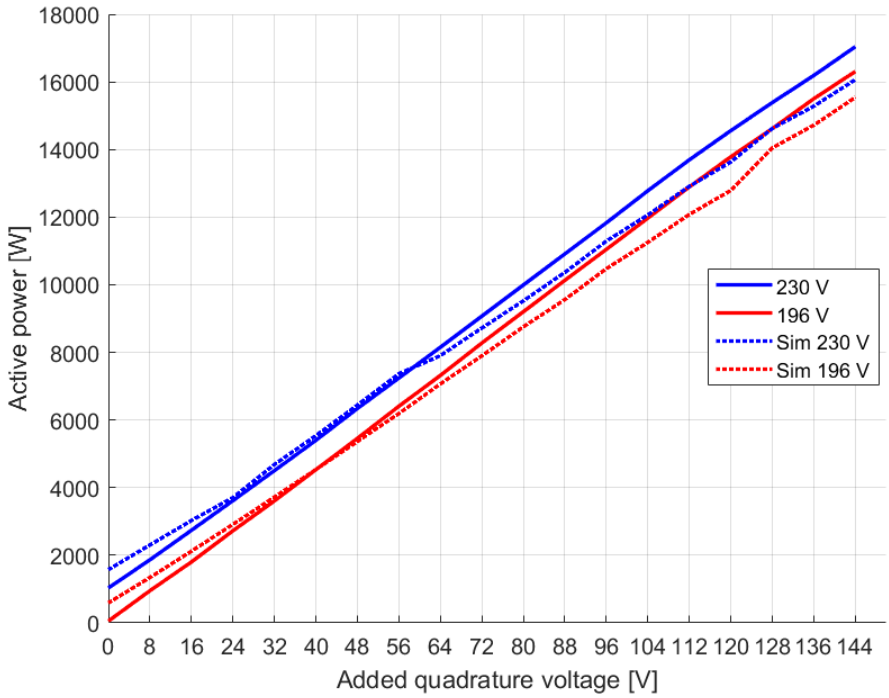

Figure 13. The active power transfer through the 22 sections transmission line for laboratory measurements (line) and simulations (dotted line).

In both cases, the low added quadrature voltage values result in higher power transfer simulations than real tests. However, for the high voltage values (more than 88 V), there is a noticeable active power difference. The differences result from both inaccuracies in laboratory parameter measurements (e.g., short-circuit power for based voltage, transformer parameters, transformer and transmission line connection resistances) and inaccuracy in the simulation solution. However, the tendency and active power value level are kept. As a confirmation, output voltage values obtained from the simulation model are presented (Table 4).

Table 4. The ACPST output voltages for 230 V and 196 V longitudinal voltages.

Quad. Voltage [V]	**0**	**8**	**16**	**24**	**32**	**40**	**48**	**56**	**64**	**72**
Output ACPST voltage [V] (blue dotted case 230 V)	230.6	230.2	229.4	228.2	231.5	232.9	234.8	237.4	233.6	234.8
Output ACPST voltage [V] (red dotted case 196 V)	211.2	210.9	210.8	210.9	211.3	211.9	212.7	213.7	214.8	216.2
Quad. Voltage [V]	**80**	**88**	**96**	**104**	**112**	**120**	**128**	**136**	**144**	
Output ACPST voltage [V] (blue dotted case 230 V)	236.3	237.8	239.7	241.5	243.6	245.6	244.9	246.6	248.5	
Output ACPST voltage [V] (red dotted case 196 V)	217.8	219.5	221.2	223.3	225.3	227.4	229.3	231.6	233.8	

By comparing ACPST output voltages—some differences in their values are visible, but they are not too big. For the blue case, 0 V, there is a 1.7% difference; 144 V is 2.5% and the red case gives differences of 1.1% and 1.7%, respectively. Therefore, the obtained results are acceptable to the next part—verification of transferred active power in cases of classical APST and the proposed ACPST model.

6. The ACPST and APST Power Transfer Comparative Analysis

The presented ACPST construction is, without a doubt, a more expensive solution. However, there are analyzed features of the proposed unit for this research stage and potential benefits in the power flow control. For the nominal input voltage to the APST, higher power flows can be observed for the same added quadrature voltage. This is the consequence of a smaller impedance contributing to the system because there is no additional transformer responsible for longitudinal voltage (as in ACPST). Power flows for nominal line voltage supplying both PSTs are presented in Figure 14.

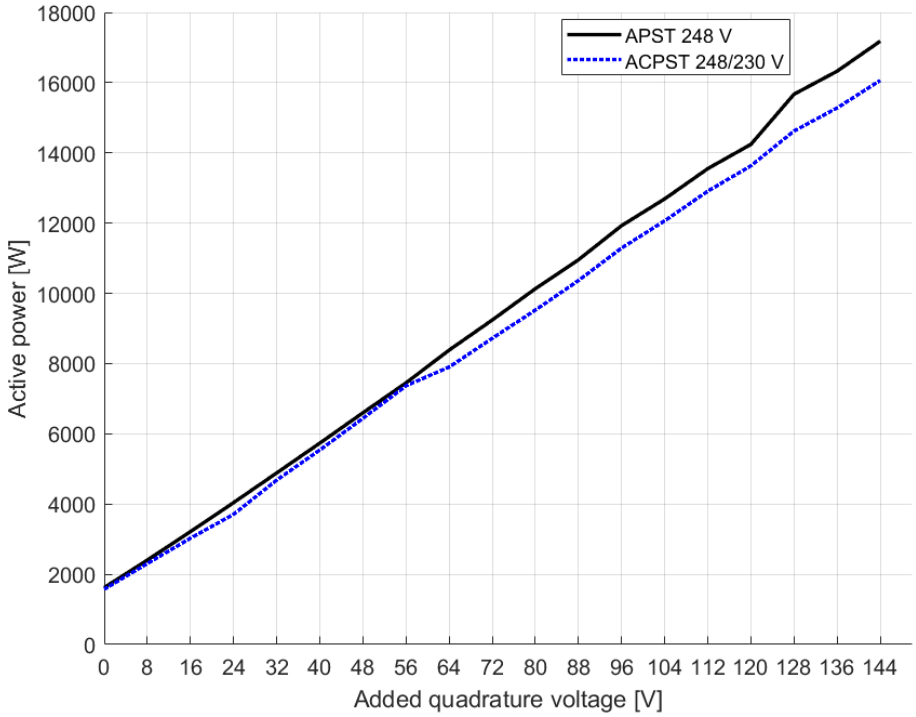

Figure 14. The active power transfer through the 22 sections line with APST (black) and ACPST (blue dotted).

For the ACPST, longitudinal voltage regulation from 248 V input value to 230 V was used. However, for APST, there was no possibility of achieving that effect, so for the presented active power flows, it is necessary to show and correlate output voltages for both cases. The compared values are collected in Table 5.

Table 5. The output voltages for APST and ACPST comparison.

Quad. Voltage (V)	**0**	**8**	**16**	**24**	**32**	**40**	**48**	**56**	**64**	**72**
Output ACPST voltage (V) (248/230 V)	230.6	230.2	229.4	228.2	231.5	232.9	234.8	237.4	233.6	234.8
Output APST voltage (V)	245.9	245.7	245.7	245.9	246.3	246.8	247.6	248.5	248.6	250.8
Quad. Voltage (V)	**80**	**88**	**96**	**104**	**112**	**120**	**128**	**136**	**144**	
Output ACPST voltage (V) (blue case 230 V)	236.3	237.8	239.7	241.5	243.6	245.6	244.9	246.6	248.5	
Output APST voltage (V)	252.2	253.6	255.3	256.8	258.6	260.1	262.9	264.5	266.5	

The same added quadrature voltage from 0 to 56 V results in almost the same active power transfer. For higher added voltage values, the APST enables sending from 0.5 kW (64 V added) to 1.1 kW (144 V added). However, gained profits in the transmitted power are occupied by the elevated output PST voltage (0 V added results 15 V higher output voltage, 64 V added −15 V higher output voltage, 144 V added −18 V higher output voltage). In this way, APST cannot be implemented in real-life systems for cases of relatively high input voltage values, because, for this situation, its output voltage can be too high and overrun maximal line voltage (what comes from the line insulation conditions).

The proposed ACPST allows achieving comparative power transfer while keeping output voltage values in the range limited by the transmission system operator (TSO) requirements.

7. Conclusions

In this article, the asymmetrical phase shifting transformers (APST) are described. Conventional APST solutions are compared to the proposed asymmetrical controllable phase shifting transformer (ACPST) and their ability to control power flows in the transmission power lines.

Classical APST is, first of all, a cheaper solution, which is essential for the investor. However, for some reasons, the APST price cannot be the most decisive during the planning stage because of the advantages of ACPST. The authors proposed that PST provides much more possibilities to control system power flows, which come from additional longitudinal voltage regulation. Due to this, the same power flows can almost be achieved, but for much lower output voltage levels. The construction of the output voltage phasor is a direct result from the triangle dependencies. For ACPST—there was the ability to gain output voltage from the equilateral triangle or even add the quadrature voltage higher than the longitudinal voltage (e.g., longitudinal voltage 196 V and quadrature one 200 V). In this way, obtaining phase angle shifting for no-load is greater. In the laboratory set-up, the phase angle is greater at c.a. 7° comparing to APST.

The ACPST construction allows using different regulation methods, e.g., for constant PST output voltage. In this way, the power transfer can be magnified via longitudinal and quadrature voltage regulation without unnecessary output voltage growth, like in the classical APST constructions. This fact is a significant advantage.

The presented ACPST unit can be installed in the power systems with high renewable energy source penetration, where the electrical energy parameters can vary very fast. Using ACPST properties in such systems—both voltage values and transferred power can be adjusted to achieve local system stability and the renewable energy production maximization, as well.

The next step in ACPST research is to improve the construction of the presented PST idea. In this article, the laboratory's two-transformer set was implemented to observe and research possible advantages of such a solution without any discussion about constructional issues. The proposed solutions are now reported in a patent application at the Polish Patent and Trademark Office.

To conclude, ACPST operation in power systems bring better effects than classical asymmetrical phase shifting transformers. It provides more flexible control abilities for adjusting both output voltage and phase angle and, as a result, transferred power.

The main disadvantage of this PST type is the necessity of at least two transformer unit usages—the first one to adjust longitudinal voltage and the second one to adjust quadrature voltage.

Author Contributions: Conceptualization, P.A. and J.S.; methodology, P.A. and J.S.; software, P.A.; validation, J.S.; formal analysis, P.A. and J.S.; investigation, P.A.; resources, J.S.; data curation, P.A.; writing—original draft preparation, P.A. and J.S.; writing—review and editing, J.S.; visualization, P.A.; supervision, J.S. All authors have read and agreed to the published version of the manuscript.

Funding: This research was funded by Polish Ministry of Science and Higher Education and performed by the Department of Electrical Engineering (E2) of Cracow University of Technology.

Institutional Review Board Statement: Not applicable.

Informed Consent Statement: Not applicable.

Conflicts of Interest: The authors declare no conflict of interest.

References

1. Adapa, R.; Nilsson, S.; Andersen, B.; Yang, Y. Technical Description of the Unified Power Flow Controller (UPFC) and Its Potential Variations. In *Flexible AC Transmission Systems*; Andersen, B., Nilsson, S., Eds.; CIGRE Green Books; Springer: Cham, Switzerland, 2020. [CrossRef]
2. Relić, F.; Marić, P.; Glavaš, H.; Petrović, I. Influence of FACTS Device Implementation on Performance of Distribution Network with Integrated Renewable Energy Sources. *Energies* **2020**, *13*, 5516. [CrossRef]
3. Ćalasan, M.; Konjić, T.; Kecojević, K.; Nikitović, L. Optimal Allocation of Static Var Compensators in Electric Power Systems. *Energies* **2020**, *13*, 3219. [CrossRef]
4. Bruno, S.; De Carne, G.; La Scala, M. Distributed FACTS for Power System Transient Stability Control. *Energies* **2020**, *13*, 2901. [CrossRef]
5. Sieńko, T.; Szczepanik, J.; Martis, C. Reactive Power Transfer via Matrix Converter Controlled by the "One Periodical" Algorithm. *Energies* **2020**, *13*, 665. [CrossRef]
6. Joint Study Joint Study by ČEPS, MAVIR, PSE and SEPS Regarding the Issue of Unplanned Flows in the CEE Region in Relation to the Common Market Area Germany—Austria. January 2013. Available online: https://www.pse.pl/documents/20182/51490/Unplanned_flows_in_the_CEE_region.pdf/44c6534e-a30d-4f06-9f7e-cb941b0ccf40 (accessed on 25 March 2021).
7. Urząd Regulacji Energetyki. *Sprawozdanie z Działalności Prezesa URE w 2019r*; Urząd Regulacji Energetyki: Warszawa, Poland, 2020.
8. Singh, A.; Frei, T.; Chokani, N.; Abhari, R.S. Impact of Unplanned Power Flows in Interconnected Transmission Systems—Case Study of Central Eastern European Region. *Energy Policy* **2016**, *91*, 287–303. [CrossRef]
9. Verboomen, J.; Van Hertem, D.; Schavemaker, P.H.; Kling, W.L.; Belmans, R. Phase shifting transformers: Principles and applications. In Proceedings of the 2005 International Conference on Future Power Systems, Amsterdam, The Netherlands, 16–18 November 2005; p. 6. [CrossRef]
10. Van Hertem, D. The Use of Power Flow Controlling Devices in the Liberalized Market. Ph.D. Thesis, K.U. Leuven, Leuven, Belgium, 2009.
11. Kling, W.; Klaar, D.; Schuld, J.; Kanters, A.; Koreman, C.; Reijnders, H.; Spoorenberg, C. *Phase Shifting Transformers Installed in The Netherlands in Order to Increase Available International Transmission Capacity*; CIGRE C2-207; CIGRE: Paris, France, 2004.
12. Korab, R.; Owczarek, R. Cross-Border Power Flow Control by Using Phase Shifting Transformers. *Przeglad Elektrotechniczny* **2012**, *88*, 299–302.
13. Kocot, H.; Korab, R.; Owczarek, R.; Przygrodzki, M.; Żmuda, K. *Countermeasures for Dealing with Uncheduled Power Flows within an Interconnected Power System*; Elektryka: Szczecin, Poland, 2015.
14. European Network of Transmission System Operators for Electricity. *TYNDP 2020 Main Report*; Version for ACER Opinion; European Network of Transmission System Operators for Electricity: Brussels, Belgium, 2021.
15. European Network of Transmission System Operators for Electricity. *Regional Investment Plan Northern Seas*; Draft Version Prior to Public Consultation; European Network of Transmission System Operators for Electricity: Brussels, Belgium, 2020.

16. European Network of Transmission System Operators for Electricity. *Regional Investment Plan CCE*; Draft Version Prior to Public Consultation; European Network of Transmission System Operators for Electricity: Brussels, Belgium, 2020.
17. Ohki, Y. Construction of a new phase-shifting transformer [News from Japan]. *IEEE Electr. Insul. Mag.* **2016**, *32*, 44–47. [CrossRef]
18. Szczepanik, J. *The Multiphase Matrix Converter for Power System Applications*; Monograph, Electrical and Computer Engineering; Cracow University of Technology: Kraków, Poland, 2014.
19. Lubośny, Z.; Machowski, J. *Power System Stability*; WNT: Warszawa, Poland, 2018. (In Polish)
20. Machowski, J. *Power System Control*; Oficyna Wydawnicza Politechniki Warszawskiej: Warszawa, Poland, 2017. (In Polish)
21. *IEEE Guide for the Application, Specification, and Testing of Phase-Shifting Transformers*; IEEE Std C57.135-2011 (Revision of IEEE Std C57.135-2001); IEEE: New York, NY, USA, 2011; pp. 1–50. [CrossRef]
22. European Network of Transmission System Operators for Electricity. Phase Shift Transformer Modelling; Version 1.0.0. CGMES V2.4.14. Available online: https://eepublicdownloads.entsoe.eu/clean-documents/CIM_documents/Grid_Model_CIM/ENTSOE_CGMES_v2.4_28May2014_PSTmodelling.pdf (accessed on 25 March 2021).
23. European Network of Transmission System Operators for Electricity. Phase Shifting Transformers (PST). Available online: https://www.entsoe.eu/Technopedia/techsheets/phase-shifting-transformers-pst (accessed on 26 March 2021).
24. Siemens Energy. Phase Shifter Application Workshop. PJM Power Pool. March 2015. Available online: https://pjm.com/-/media/committees-groups/task-forces/partf/20150514/20150514-item-03-pjm-phase-shifting-transformer-principles.ashx (accessed on 25 March 2021).
25. Bednarczyk, T.; Szablicki, M.; Halinka, A.; Rzepka, P.; Sowa, P. Phase Shifting Transformer Electromagnetic Model Dedicated for Power System Protection Testing in a Transient Condition. *Energies* **2021**, *14*, 627. [CrossRef]
26. Sakallıoğlu, B.; Esenboğa, B.; Demirdelen, T.; Tümay, M. Performance evaluation of phase-shifting transformer for integration of renewable energy sources. *Electr. Eng.* **2020**, *102*, 2025–2039. [CrossRef]
27. Mamcarz, D.; Albrechtowicz, P.; Radwan-Pragłowska, N.; Rozegnał, B. The Analysis of the Symmetrical Short-Circuit Currents in Backup Power Supply Systems with Low-Power Synchronous Generators. *Energies* **2020**, *13*, 4474. [CrossRef]
28. Rozegnał, B.; Albrechtowicz, P.; Mamcarz, D.; Radwan-Pragłowska, N.; Cebula, A. The Short-Circuit Protections in Hybrid Systems with Low-Power Synchronous Generators. *Energies* **2021**, *14*, 160. [CrossRef]
29. Szczepanik, J.; Rozegnał, B. The development of the real life model of the five node power system. *Czasopismo Techniczne Elektrotechnika Y* **2015**, *112*, 83–102.